Dalton Transactions

RSC Publishing

PAPER

View Article Online
View Journal | View Issue

Cite this: *Dalton Trans.*, 2013, **42**, 4931

The first bis-cyanoxime: synthesis and properties of a new versatile and accessible polydentate bifunctional building block for coordination and supramolecular chemistry†

Carl Cheadle,[a] Nikolay Gerasimchuk,*[a] Charles L. Barnes,[b] Sergiy I. Tyukhtenko[c] and Svitlana Silchenko[d]

A new multidentate bifunctional organic ligand – di-*N*,*N*′-(2-cyano-2-oximinoacetyl)piperazine – was synthesized in high yield using a two-step procedure carried out under ambient conditions. At first, the reaction of piperazine and neat methylcyanoacetate led to the di-*N*,*N*′-(cyanoacetyl)piperazine (**1**), which then was converted into bis-cyanoxime, di-*N*,*N*′-(2-cyano-2-oximinoacetyl)piperazine (HL, **2**) using a room temperature nitrosation reaction with gaseous methylnitrite. Synthesized bis-cyanoxime was characterized by ^{1}H, ^{13}C NMR, UV-visible, IR spectroscopy and the X-ray analysis. The ligand **2** exists as a mixture of three diastereomers arising from the *syn*- and *anti*-geometry of the cyanoxime group. The prolonged crystallization of **2** from an ethanol–water mixture leads to the formation of: (a) colorless crystals that according to the X-ray analysis contain a 51.2 : 48.8% co-crystallized mixture of both isomers that have the same H-bonding motif (minority), and (b) a white amorphous material that represents an almost pure *anti*-isomer (majority). The deprotonation of **2** leads to the formation of a yellow dianion that demonstrated pronounced solvatochromism of its n → π* transition in the nitroso-chromophore. The di-sodium salt $Na_2L{\cdot}4H_2O$ (**3**) was obtained from **2** using $NaOC_2H_5$ in ethanol. The new bis-cyanoxime **2** reacts with Tl_2CO_3 and $AgNO_3$ in aqueous solutions with the formation of light-stable, sparingly soluble yellow precipitates of $M'_2L{\cdot}xH_2O$ composition (M′ = Tl, Ag; Tl = **4**, *x* = 0; Ag = **5**, *x* = 2). The reaction of **3** with Ni^{2+} or $K_2M''Cl_4$ (M″ = Pd, Pt) in aqueous solutions leads to $NiL{\cdot}4H_2O$ (**6**), $PdL{\cdot}4H_2O$ (**7**) and $PtL{\cdot}5H_2O$ (**8**). The crystal structure of **4** was determined and revealed the formation of a 3D-coordination polymeric complex in which the bis-cyanoxime acts as a dianionic, bridging, formally decadentate ligand. Each Tl(I) center has two bonds (2.655, 2.769 Å), shorter than the sum of ionic radii Tl–O (oxime group), and three longer, >2.89 Å, mostly electrostatic Tl···O contacts, involving oxygen atoms of the amide-group and the oxime-group of neighboring units. Among several possible binding modes, the coordination of the bis-cyanoxime dianion of **2** adopted in complex **4** is unusual, and evidenced its great potential as a versatile building block for coordination and supramolecular chemistry.

Received 23rd August 2012,
Accepted 6th January 2013

DOI: 10.1039/c2dt31924a

www.rsc.org/dalton

[a]*Department of Chemistry, Temple Hall 432, Missouri State University, Springfield, MO 65897, USA. E-mail: NNGerasimchuk@MissouriState.edu; Tel: +(417) 836-5165*
[b]*Department of Chemistry, University of Missouri-Columbia, 125 Chemistry Building, Columbia, MO 65211, USA*
[c]*Center for Drug Discovery, 116 Mugar Hall, Northeastern University, 360 Huntington Ave, Boston, MA 02115, USA*
[d]*Absorbtion Systems Inc., 440 Creamy Way, S.300, Exton, PA 19341, USA*

†Electronic supplementary information (ESI) available: The list of structurally and spectroscopically characterized non-chelating dioximes (ESI 1); the list of currently known and studied cyanoximes (ESI 2); details of the structure solution and refinement of **2** (ESI 3); details of the structure solution and refinement of **4** (ESI 4,5); checkCIF report for the structure of **2** (ESI 6); checkCIF report for the structure of **4** (ESI 7); the actual experimental setup used for the generation of methyl nitrite for the nitrosation of acetonitriles under basic conditions (ESI 8); tables of variable temperature ^{1}H, $^{13}C\{^{1}H\}$ NMR chemical shifts for **2** (ESI 9,10); actual microscope photographs of samples of **4–8** at 40× magnification (ESI 11); actual photographs of spontaneously resolved crystals of the isomeric mixture and individual component of **2** (ESI 12); geometrical isomers of **2** in relations to $^{13}C\{^{1}H\}$ NMR spectra (ESI 13); $^{13}C\{^{1}H\}$ NMR spectra of a co-crystallized mixture of the *syn*-/*anti*-isomers (51.2% : 48.8%), and almost pure *anti*-isomer (ESI 14); overlaid NMR spectra of the disodium salt **3** in DMSO-d_6 at different temperatures (ESI 15); geometrical isomers of **2** and charge delocalization in the dianion of **2** (ESI 16); packing diagram of **2** and table of H-bonding in the structure (ESI 17); fragments of the crystal structures of other cyanoximes that demonstrate the coexistence of two geometrical isomers in the same unit cell (ESI 18–23); a picture of a large Dewar flask used for a slow crystallization of hot solutions of **4** (ESI 24); details of geometry of two adjacent Tl_2O_2 rhombs in the structure of **4** and coordination polyehedron of Tl(I) in the complex (ESI 25). CCDC 897457 and 897458. For ESI and crystallographic data in CIF or other electronic format see DOI: 10.1039/c2dt31924a

Introduction

The chemistry and application of bifunctional ionizable ligands received considerable attention in the last decade due to a large variety of different lattice architectures found in numerous crystal structures of transition and main group metal complexes. Aliphatic and aromatic carboxylic acids and diacids were the main ligands in shaping the concept of the metal–organic frameworks (MOFs) and coordination polymers.[1] The most common MOF forming ligands **A–E** are shown in Scheme 1 and represent isomeric phthalic acids and pyridine dicarboxylates, *etc*.

Other interesting bifunctional weak acids are dioximes. Traditional α-dioximes were found to have numerous applications in analytical chemistry,[2] coordination/organometallic chemistry,[3] molecular electronics,[4] and materials research,[5] mainly due to their ability to form stable complexes with basically any metal ion. The best-known α-dioximes are glyoximes **I**, **J** such as famous DMG, and their derivative **K**,[6] **L**,[7] for example, and 1,2-cyclohexanedion-dioxime **F** (Nioxime) with its closest analogs **G**, **H**,[8] 1,2-benzoquinonedioxime **M**[9] (BQD) and its hydrophobic derivative **N** (Scheme 1). All these α-dioximes act as powerful chelating agents.[2,3b] However, due to their structures, α-dioximes did not exhibit a great variety of binding modes or lattice architectures. Also, there are several non-chelating dioximes known which received no attention as ligands for coordination and supramolecular chemistry, but were spectroscopically and structurally characterized (ESI 1†). In the late 1970s a new class of ampolydentate ligands – cyanoximes that have the general formula NC–C(=NOH)–R – has emerged (ESI 2†). The introduction of diverse R-groups (such as CN-, amide-, thioamide-, keto-, aryl and 2-heteroaryl) into the structures of cyanoximes leads to a possibility of fine-tuning electronic and steric properties of these ligands.[10] It has been shown that cyanoximes are able to form stable main group metals and transition metal complex compounds as well as coordination polymers.[11] The chemistry of cyanoximes and their metal complexes has received considerable attention due to the spectrum of their useful properties, such as solvatochromism,[12] biological activity,[13] structural diversity[11,14,15] and remarkable light stability of Ag(I) coordination polymers.[11,16]

Despite extensive publications and presentations on cyanoximes, no bis-cyanoximes were known prior to this study. In the present work we report the first preparations and a detailed characterization of a new bis-cyanoxime ligand – di-*N*,*N*′-(2-cyano-2-oximinoacetyl) piperazine, **2**, and its several metal complexes (Scheme 2).

Experimental part

All starting compounds such as methylcyanoacetate, piperazine free base, silver(I) nitrate, thallium(I) carbonate, sodium nitrite (Aldrich, Fluka) and HPLC-grade organic solvents (Spectrum Chemicals, J.T. Baker) were used without additional purification. Melting points or decomposition temperatures for synthesized compounds were determined using the Mel-Temp apparatus (Thomas Hoover). The TLC for the ligand and its precursor were carried out on silica-coated glass plates (Merck), containing a 256 nm fluorescent indicator. Elemental analyses on C,H,N content were performed at the Atlantic

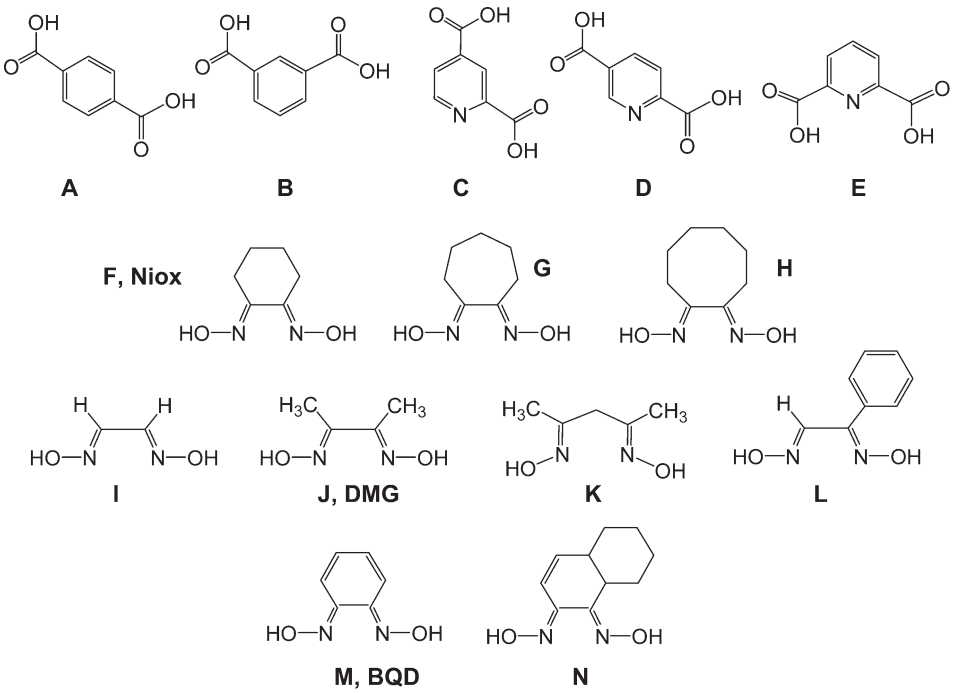

Scheme 1

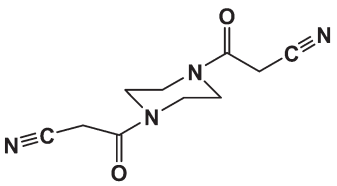

1

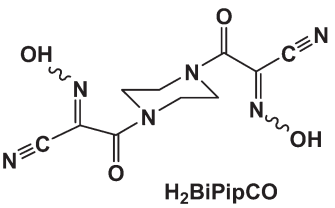

H_2BiPipCO
2

Na_2BiPipCO x $4H_2O$
3

Tl_2BiPipCO
4

Ag_2BiPipCO x $2H_2O$
5

NiBiPipCO x $4H_2O$
6

PdBiPipCO x $4H_2O$
7

PtBiPipCO x $5H_2O$
8

Scheme 2

Microlab (Norcross, GA). The electrical conductivity of 1 mM solutions of Na_2(BiPipCO) (**3**) and Tl_2(BiPipCO) (**4**) in water was measured at 295 K, using the YSI Conductance-Resistance meter Model 34. Solutions of KBr and K_2SO_4 (as 1 : 1 and 1 : 2 types of electrolytes respectively) were used for the electrode calibration, since thallium(I) compounds resemble those for potassium.[17]

Spectroscopy

The bis-cyanoxime **2** was characterized by ^{1}H, ^{13}C NMR, COSY and HMQC spectroscopy (solutions in DMSO-d_6; TMS was an internal standard; Varian INova 400 MHz spectrometer; variable temperature studies in the range of +25–+95 °C). The UV-visible spectra of the protonated ligand H_2BiPipCO, **2**, and its di-Na^+ salt **3** were recorded at room temperature (293 K) using an HP 8354 spectrophotometer in the range 200–1100 nm, in 1 mm and 10 mm quartz cuvettes (Starna Inc.). Infrared spectra were recorded in the range 500–4000 cm^{-1}, using the FT IR Nicolet Magna 550 spectrophotometer in a KBr matrix for the protonated cyanoxime **2**. However, the IR spectra of **4** and **5** were obtained from mulls in Nujol, to avoid solid state exchange reactions between KBr and monovalent Tl and Ag complexes during the pellet preparation.

X-Ray crystallography

Suitable single crystals of the bis-cyanoxime **2** and its di-Tl-complex **4** were positioned in a cryo-loop on the goniometer head of the Bruker APEX 2 diffractometer equipped with a SMART CCD area detector. Data sets were measured at 120 K. The intensity data were collected in ω scan mode using the Mo tube (Kα radiation; λ = 0.71073 Å) with a highly oriented graphite monochromator. Intensities were integrated from 4 series of 364 exposures, each covering 0.5° in ω at 20 seconds of acquisition time, with the total data set being a sphere.[18] The space group determination was done with the aid of XPREP software.[19] The absorption correction was performed using the SADABS program that was included in the Bruker AXS software package.[20] Both structures were solved by direct methods and refined by least squares on weighted F^2 values for all reflections using the SHELXTL program. The bis-cyanoxime **2** forms well-shaped, but small, prism-type crystals that have a very high propensity for twinning. Thus, one of the best-selected crystal specimens of **2**, in fact, turned out to be a non-merohedral twin. Details of the solution and refinement for this compound can be found in ESI 3.† Hydrogen atoms of C–H origin in the structures of H_2BiPipCO (**2**) and Tl_2(BiPipCO) (**4**) were placed in their idealized geometrical positions and refined isotropically in a riding scheme, while oxime hydrogens O–H were clearly identified on a difference map. Some important details of the structure determination for the metal complex **4** are presented in ESI 4.† We should mention that in the Tl-complex **4** we observed several Q-peaks of residual electron density on the difference map at distances ~1 Å from the metal center (ESI 5†). The largest one is equal to 2.78 e $Å^{-3}$ at a distance of 0.93 Å, and cannot be matched with any meaningful atom or contact. Such electron density "ripples" near thallium (Z = 81) are typical of the compounds of heavy elements. Especially this is the case when single crystals have relatively high mosaicity and imperfections, such as micro-cracks and opacity. The latter was the case suitable for the X-ray analysis of single crystals of **4**. The final analysis of the variance between observed and calculated structure factors showed no apparent errors. The crystal data for compounds **2** and **4** are presented in Table 1, while bond lengths and valence angles are summarized in Table 2. Figures for the crystal structures of these complexes were drawn using Mercury 4.1.2 and ORTEP 32 software[21] at a 50% thermal ellipsoids probability level. The PLATON checks of crystallographic data and actual CIF files for the reported structures can be found in the ESI 6,7.† CCDC numbers: 897458 (**2**, H_2BiPiPCO) and 897457 (**4**, Tl_2BiPiPCO).

Determination of pK_a value for synthesized di-*N*,*N*′-(2-cyano-2-oximinoacetyl)piperazine 2

Studies were carried out using a Sirius Analytical Instruments automated titration station (Sussex, UK) equipped with a

Table 1 Crystal data for studied compounds

Compound	H_2BiPipCO, **2**	Tl_2(BiPipCO), **4**
Empirical formula	$C_{10}H_{10}N_6O_4$	$C_5H_4N_3O_2Tl$
Formula weight	278.24	684.96
Temperature (K)	120(2)	120.2(2)
Wavelength (Å)	0.71073 (Mo)	0.71073 (Mo)
Crystal system	Monoclinic	Monoclinic
Space group	$P2(1)/n$; #14	$P2(1)/c$; #14
Unit cell dimensions (A/°)	a = 6.298(5)	a = 4.2757(8)
	b = 15.488(12)	b = 13.674(2)
	c = 6.453(5)	c = 12.009(2)
	α = 90	α = 90
	β = 102.648(13)	β = 99.338(2)
	γ = 90	γ = 90
Volume (Å^3)	614.2(8)	698.69(19)
Z	2	2
Density (calc.) (Mg m^{-3})	1.505	3.284
Absorption coefficient (μ) (mm^{-1})	0.120	23.258
F(000)	288	608
Crystal size (mm)	0.13 × 0.08 × 06	0.18 × 0.10 × 0.07
Index ranges	−7 < = h < = 7	−5 < = h < = 5
	0 < = k < = 19	−17 < = k < = 17
	0 < = l < = 7	−15 < = l < = 15
Reflections collected	1237[a]	8049
Independent reflections	1237 [R(int) = 0.0780]	1555 [R(int) = 0.0425]
Completeness to Θ (%)	26.34° (99.7%)	27.21° (99.6%)
Data/restraints/parameters	1237/20/112	1555/18/100
GOF on F^2	1.091	1.272
Final R indices [$I > 2\sigma(I)$]	R_1 = 0.0627, wR_2 = 0.1757	R_1 = 0.0451, wR_2 = 0.0987
R indices (all data)	R_1 = 0.0880, wR_2 = 0.1921	R_1 = 0.0514, wR_2 = 0.1013
Largest difference peak and hole (e Å^{-3})	0.321 and −0.201	2.775 and −3.146

[a] Number for a major twin component used for structure solution and refinement.

Table 2 Selected bond lengths (Å) and valence angles (°) in structures of **2** and **4**

H_2BiPipCO, **2**

Bonds		Angles	
C(1)–N(1)	1.270(8)	N(1)–C(1)–C(2)	106.1(5)
C(1)–N(1A)	1.296(2)	N(1A)–C(1)–C(2)	131.6(4)
C(1)–C(2)	1.435(5)	N(1)–C(1)–C(3)	136.8(4)
C(1)–C(3)	1.499(4)	N(1A)–C(1)–C(3)	111.8(5)
C(2)–N(2)	1.137(5)	N(2)–C(2)–C(1)	178.5(4)
C(3)–O(2)	1.239(3)	O(2)–C(3)–N(3)	125.2(3)
C(3)–N(3)	1.327(4)	C(3)–N(3)–C(4)	125.6(2)
C(4)–N(3)	1.465(4)	C(3)–N(3)–C(5)	120.6(2)
C(5)–N(3)	1.468(4)	C(4)–N(3)–C(5)	113.5(2)
C(5)–C(4)#1[a]	1.511(4)	C(1)–N(1)–O(1)	106.1(6)
N(1A)–O(1A)	1.364(2)	C(1)–N(1A)–O(1A)	105.8(8)
O(1)–N(1)	1.346(8)	N(1A)–O(1A)–H(1A)	109.5
O(1)–H(1)	0.8400	N(1)–O(1)–H(1)	109.4

Tl_2(BiPipCO), **4**

Bonds		Angles	
C(1)–N(1)	1.304(16)	N(1)–C(1)–C(2)	120.2(10)
C(1)–C(2)	1.447(16)	N(1)–C(1)–C(3)	126.8(11)
C(1)–C(3)	1.499(15)	C(2)–C(1)–C(3)	113.1(10)
C(2)–N(2)	1.139(16)	N(2)–C(2)–C(1)	177.0(14)
C(3)–O(2)	1.258(14)	O(2)–C(3)–N(3)	121.9(10)
C(3)–N(3)	1.319(15)	C(1)–N(1)–O(1)	117.0(10)
C(4)–N(3)	1.483(14)	C(3)–N(3)–C(4)	119.6(10)
C(5)–N(3)	1.475(14)	C(3)–N(3)–C(5)	129.1(10)
N(1)–O(1)	1.307(13)	C(4)–N(3)–C(5)	111.2(9)
O(1)–Tl(1)	2.653(9)	N(1)–O(1)–Tl(1)	98.8(7)
O(1)–Tl(1)#2[b]	2.766(9)	N(1)–O(1)–Tl(1)#2[b]	149.2(8)
		Tl(1)–O(1)–Tl(1)#2	107.4(3)
		O(1)–Tl(1)–O(1)#2	72.6(3)

Symmetry transformations used to generate equivalent atoms: [a] #1 −x + 2, −y + 1, −z + 2. [b] #2 −x, −y + 1, −z + 1.

temperature-controlled bath. Since protonated bis-cyanoxime **2** is poorly soluble in water, all measurements were conducted in mixed solvent systems using DMSO as a solubilizing co-solvent. Atenolol™ and Lidocaine™ (from Aldrich) were used to calibrate the instrument. Measurements consisted of the three-step multi-stage titration in water–ethanol mixtures from 10 wt% to 20 wt% with ionic strength adjusted to 0.165 with KCl. The values were extrapolated to "zero" ethanol content to obtain an aqueous pK_a value using the Yasuda–Shedlovsky procedure. The pH in titration experiments ranged from 3 to 11.

Synthesis of compounds

Di-*N*,*N*′-(cyanoacetyl)piperazine (1) and its bis-cyanoxime (2)

Since these compounds have never been prepared before, the following experimental procedures describe their synthesis in detail. Thus, the preparation of **2** was done according to the procedures depicted in Scheme 3 from the respective substituted bis-acetonitrile precursor **1**. Hence, 2.017 g (23.4 mmol) of piperazine were dissolved in 15 mL CH_2Cl_2 and mixed with 4.4 mL (49.7 mmol) of methyl cyanoacetate in a 250 mL round-bottom flask, by stirring at room temperature under nitrogen. After ~10 h of stirring, a very thick white paste of **1** was obtained. The product was triturated with 15 mL of diluted HCl (1 : 5, by volume) to remove the unreacted piperazine. The solid residue was filtered, washed with cold water and then dried overnight using an oil vacuum pump. The yield = 4.219 g (82%) of a white solid. The compound decomposes at 215–232 °C. The TLC R_f = 0.27 in ethylacetate : acetone = 9 : 1 mobile phase. The preparation of **2**, H_2BiPipCO, was accomplished by nitrosation of **1** under basic conditions using gaseous methylnitrite, CH_3ONO, generated *via* reaction of $NaNO_2$ with a cold CH_3OH–H_2SO_4 mixture (Scheme 3 and ESI 8†). Thus, 0.303 g of sodium metal (13.2 mmol) was dissolved in 80 mL of 2-propanol under nitrogen. Once the sodium was completely dissolved, 1.221 g (5.5 mmol) of solid *N*,*N*′-(cyanoacetyl)piperazine **1** was added in portions to the sodium propoxide solution with vigorous stirring, forming a clear, colorless solution. Then, a flow of CH_3ONO gas was bubbled through the clear solution of *N*,*N*′-(cyanoacetyl)piperazine dianion, which quickly gained a yellow color (ESI 8†). The reaction mixture was first concentrated on a rotary evaporator to give a thick, viscous yellow sludge which was then dried under vacuum on an oil vacuum pump for ~1 h. The resulting yellow waxy solid was re-dissolved in 25 mL of water and acidified

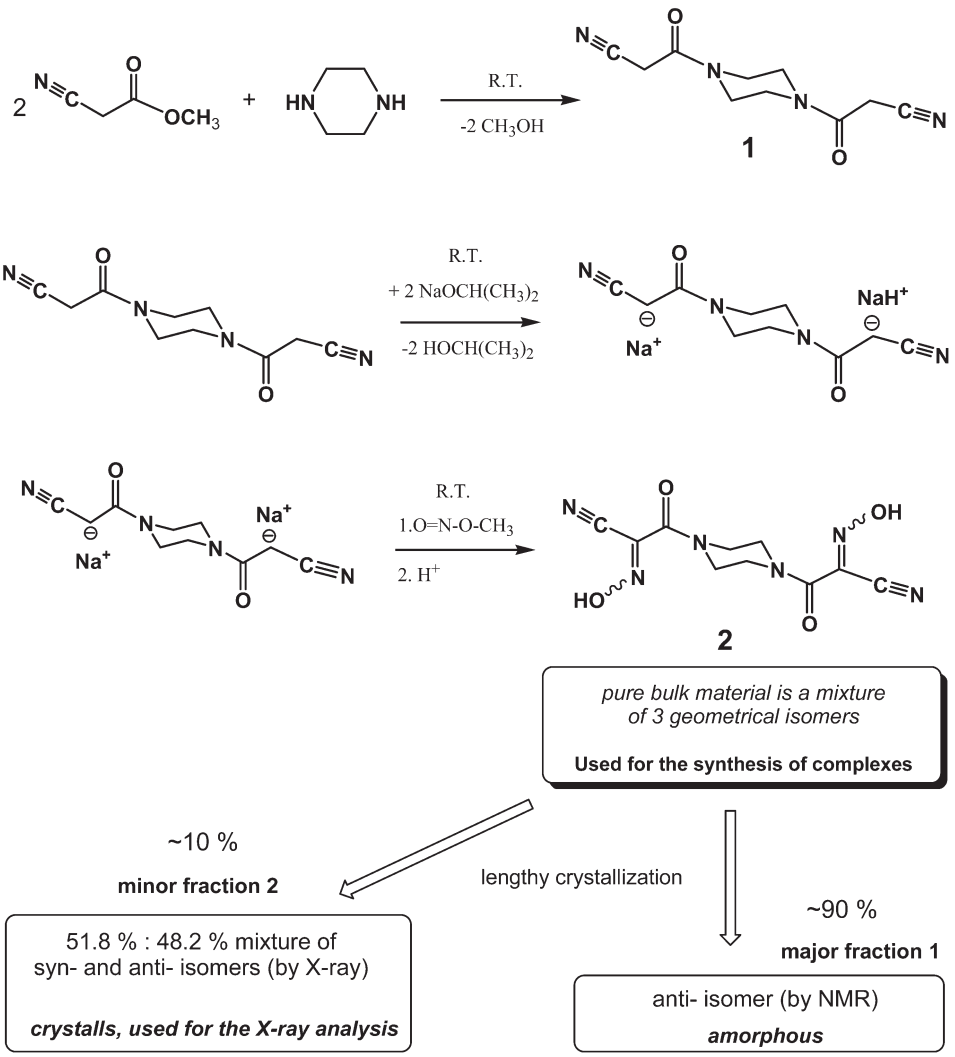

Scheme 3

dropwise to pH ~ 4 with 1.0 M HCl to give an off-white, very fine powder, poorly soluble in water. The solid was filtered and washed with warm water to result in H_2BiPipCO, **2**, which was further dried in a vacuum desiccator. The identification of **2** was done first using the TLC: co-spotting with the starting compound **1** revealed the absence of the initial compound in the product. There are three distinctive spots on the TLC plate that evidenced the presence of 3 isomers: *anti–anti*, *anti–syn*, and *syn–syn* (Scheme 4) with R_f values of 0.30, 0.41 and 0.59 respectively in ethylacetate : hexanes = 4 : 1 eluent. The yield = 1.04 g (67%); the compound decomposes in the range of 173–252 °C. For $C_{10}H_{10}N_6O_4$ calculated (found), %: C – 43.17 (42.64), H – 3.62 (3.81), N – 30.21 (28.83). Tabulated ^{1}H and ^{13}C{^{1}H} NMR spectroscopic data, including variable temperature experiments, for the compound **2** are presented in ESI 9,10.†

Preparation of metal-containing derivatives

The sodium salt – compound **3** – was prepared by the deprotonation of **2** with $NaOC_2H_5$. Thus, 0.047 g (2.0 mmol) of sodium metal was dissolved under a nitrogen flow in 50 mL of absolute ethanol to generate sodium ethoxide and then

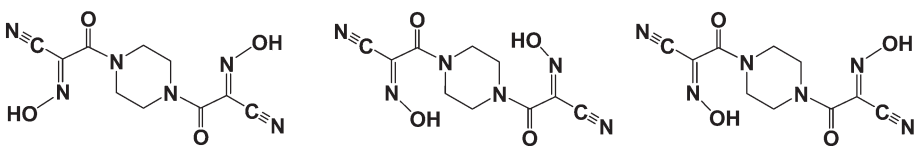

Scheme 4

0.275 g (1.0 mmol) of H_2BiPipCO was added to the ethanol solution at once, while stirring. The reaction mixture instantly changed color and was concentrated on rotovap to yield a bright yellow solid, which was further dried under vacuum. The solid **3** is highly hygroscopic and will deliquesce upon lengthy exposure to atmospheric conditions. The yield = 0.349 g (~100%), m.p. = 126–140 °C (dec). For $C_{10}H_8N_6O_4Na_2{\cdot}2H_2O$ calc. (found), %: C – 33.53 (33.89), H – 3.38 (3.41), N – 23.46 (23.26). It is soluble in water, cold DMF, DMSO and somewhat soluble in CH_3OH, but is not soluble in other common organic solvents.

For the preparation of complex **4** 0.476 g (1.0 mmol) of Tl_2CO_3 was dissolved in a minimal amount of hot deionized water (5 mL). Then, 0.141 g of solid H_2BiPipCO **2** (1.0 mmol) was added to the boiling Tl_2CO_3 solution at once, to give a bright yellow solution. The solution was quickly hot-filtered into the large-mouth test tube inserted into a Dewar flask with water preheated to 95 °C and let slowly cool for three days for the growth of crystals. Pale yellow crystals were recovered, with some of them being suitable for X-ray analysis (ESI 11†). The yield is 68%; the compound decomposes at 211–224 °C. For $C_{10}H_8N_6O_4Tl_2$ calc. (found), %: C – 17.53 (17.59), H – 1.18 (1.20), N – 12.27 (12.13). Complex **4** is soluble in water, DMF, DMSO and Py, but is insoluble in acetone, alcohols, CH_3CN and chlorohydrocarbons.

For the synthesis of complex **5** a solution of 0.51 mmol of **3** in 15 mL of water was mixed in a 50 mL Erlenmeyer flask with 0.1824 g (1.1 mmol) of $AgNO_3$ in 5 mL of deionized water at room temperature. The Ag_2BiPipCO·$2H_2O$, **5**, immediately forms a thick yellow precipitate (ESI 11†), which was filtered, washed thoroughly with deionized water and dried in a vacuum desiccator charged with H_2SO_4 (conc.). The yield = 0.2230 g (89%); the complex decomposes at 168–176 °C. For $C_{10}H_8N_6O_4Ag_2{\cdot}2H_2O$ calc. (found), %: C – 22.75 (22.77), H – 2.29 (1.87), N – 15.92 (15.51). Compound **5** is somewhat soluble in hot DMF, DMSO and Py, but it is not soluble at any temperature in common organic solvents or water.

Ni-triad complexes **6–8** were obtained in aqueous solutions under ambient conditions according to reactions 4 and 5 (see the Results and discussion section below). Thus, nickel complex **6** represents a gray powder, insoluble in water, and appears within several minutes after mixing the starting compounds (ESI 11†). For Ni complex preparation, 0.2637 g (0.94 mM) of $Ni(NO_3)_2$ in 5 mL of water were added dropwise under stirring to 15 mL of the solution of **3** (0.3016 g; 0.94 mM). Yield is 87%; the complex decomposes in the range 347–376 °C. For $C_{10}H_8N_6O_4Ni{\cdot}4H_2O$ calc. (found), %: C – 29.51 (30.30); H – 3.96 (3.80); N – 20.65 (20.24). Complex **6** has low solubility in hot DMF, DMSO and Py, and is not soluble at any temperature in common organic solvents or water.

For the preparation of Pd(II) complex **7** a solution of potassium tetrachloropalladate (0.1718 g, 0.53 mM) in 10 mL of water was added dropwise under stirring to a solution of **3** (0.53 mM) in 11 mL of water. Palladium complex **7** is a bright yellow powder that precipitates out of the solution within ~10 minutes after mixing the components (ESI 11†). The yield is ~100%; the complex decomposes in the range of 221–273 °C. For $C_{10}H_8N_6O_4Pd{\cdot}4H_2O$ calc. (found), %: C – 26.42 (26.98), H – 3.55 (2.85), N – 18.48 (18.55). Compound **7** is somewhat soluble in DMSO and Py, but is not soluble in common organic solvents or water.

For the synthesis of Pt(II) complex **8** a solution of potassium tetrachloroplatinate (0.3784 g; 0.92 mM) in 4 mL of water was added dropwise to a solution of **3** (0.92 mM) in 11 mL of water under intensive stirring. Platinum complex **8** represents a very fine, dark green-brown powder which precipitated out of the reaction mixture after ~12 h of mixing the starting compounds (ESI 11†). Yield ~100%; the compound decomposes in the range of 270–318 °C. For $C_{10}H_8N_6O_4{\cdot}5H_2O$ Pt calc. (found), %: C – 21.40 (21.50), H – 3.23 (2.64), N – 14.97 (14.62). Complex **8** is slightly soluble in hot DMSO and Py, but is not soluble at any temperature in other organic solvents or water.

Safety note: *Although we have not encountered any problems during many years of laboratory work and handling, special care should be taken during work with thallium compounds because of their high toxicity.*[22] *Both Tl(I) carbonate and cyanoximates are water-soluble compounds, and that emphasizes the absolute necessity for wearing protective gloves at all times when working with these compounds. However, no respiratory tract covers are required since Tl(I) compounds are ionic and not volatile.*

Results and discussion

Synthesis of metal-containing compounds 3–8

The di-*N*,*N*′-(2-cyano-2-oximinoacetyl)piperazine (**2**) was obtained for the first time in high yield using the nitrosation reaction of its precursor *N*,*N*′-(cyanoacetyl)piperazine with gaseous CH_3ONO under ambient conditions. This particularly facile and convenient method of introduction of the oxime group into organic compounds with non-active methylene groups has been extensively developed and recently patented by us.[23] For the characterization of the newly obtained bis-cyanoxime **2** as a ligand we obtained its di-sodium salt Na_2BiPipCO (**3**), and also respective monovalent Tl and Ag complexes **4** and **5**, and Ni-triad complexes **6–8**. Since di-*N*,*N*′-(2-cyano-2-oximinoacetyl)piperazine (**2**) is sparingly soluble in water, it cannot be efficiently used for the preparation of many pure conventional coordination compounds. On the other hand, its disodium salt **3** is well soluble in water and reacts quickly with aqueous solutions of salts of the main group elements (Tl) and transition metals (Ag, Ni-triad).

The disodium salt **3** was obtained *via* the reaction 1 in absolute ethanol:

$$H_2\text{BiPipCO} + 2NaOC_2H_5 \xrightarrow{RT} Na_2\text{BiPipCO}\downarrow + 2\ C_2H_5OH \quad (1)$$

To synthesize **4**, Tl_2BiPipCO, a reaction 2 between a saturated aqueous solution of Tl_2CO_3 and a solid ligand was

carried out:

$$H_2BiPipCO + Tl_2CO_3 \xrightarrow{+95\,^{\circ}C} Tl_2BiPipCO\downarrow + [H_2CO_3] \rightarrow CO_2\uparrow + H_2O \quad (2)$$

Compound **5**, $Ag_2BiPipCO{\cdot}2H_2O$, was synthesized in aqueous solutions according to reaction 3 using $Na_2BiPipCO$, **3**, and $AgNO_3$:

$$Na_2BiPipCO + 2AgNO_3 \xrightarrow{RT} Ag_2BiPipCO{\cdot}H_2O\downarrow + 2NaNO_3 \quad (3)$$

Ni-triad (Ni, Pd, Pt) complexes **6–8** were obtained in aqueous solutions under ambient conditions according to reactions 4 and 5:

$$Na_2BiPipCO + Ni(NO_3)_2 \rightarrow NiBiPipCO{\cdot}4H_2O\downarrow + 2NaCl \quad (4)$$

$$Na_2BiPipCO + K_2[MCl_4] \rightarrow MBiPipCO{\cdot}xH_2O\downarrow + 2NaCl + 2KCl \quad M = Pd(x = 4H_2O;\ \mathbf{7}), Pt(x = 5H_2O;\ \mathbf{8}) \quad (5)$$

All metal derivatives of a new ligand **2** were obtained in high yields and, therefore, prove its suitability for the synthesis of new series of coordination compounds.

Solutions studies: electrochemical measurements

pK_a determination and conductivity. The new bis-cyanoxime ligand **2** undergoes independent stepwise deprotonation in solutions as a weak acid:

$$H_2BiPipCO \xrightarrow{K_1} H^+ + HBiPipCO^- \xrightarrow{K_2} H^+ + BiPipCO^{2-} \quad (6)$$

Values of pK_{a1} and pK_{a2} were found to be 4.76 ± 0.02 and 5.61 ± 0.02 respectively, which are comparable to other reported cyanoximes.[24] The electrical conductivity of 1 mM solutions of Tl_2(BiPipCO) was measured to be 0.203 ± 0.007 mS, which clearly indicates the dissociation of the complex, according to eqn (7) since this value is almost twice as low as for the standard 1 : 1 electrolyte. Values of electrical conductivity for 1 mM solutions of the standard ionic compounds KBr and K_2SO_4 (at 293 K) were found to be 0.182 ± 0.004 and 0.376 ± 0.007 mS respectively.

$$Tl_2(BiPipCO) \rightarrow Tl^+ + Tl(BiPipCO)^- \quad (7)$$

This evidenced that a polymeric solid state structure of the complex is lost in the solution, which is in line with UV-visible spectroscopy studies of solutions of $Na_2BiPipCO$ and Tl_2(BiPipCO) showing practically identical spectra.

Solutions studies: spectroscopic characterization

In the following three sections we propose the explanation of rather complex results of the NMR spectroscopy. Our tentative interpretation of data and signal assignments, although suggestive and not complete, was based on variable temperature NMR spectra, literature information and data of the X-ray analysis of single crystals of **2**. As indicated in Scheme 3, bis-cyanoxime **2** was obtained as a mixture of several diastereomers at different ratios (ESI 13†). The $^{13}C\{^1H\}$ NMR spectrum showed peaks pertaining to the *anti–anti* and *syn–syn* isomers, while the *syn–anti* isomer (Scheme 4) was spectroscopically undistinguishable, similarly to the NMR spectra of individual enantiomers and racemate in achiral solvents.

NMR spectra of a bulk material of 2. Data for ^1H and $^{13}C\{^1H\}$ NMR variable temperature spectra for $H_2BiPipCO$ (**2**) in DMSO-d_6 are shown in Fig. 1–3 respectively. As mentioned before, the TLC of pure **2** shows three close spots, indicating the presence of all three geometrical isomers *syn–syn*, *syn–anti*, and *syn–anti* (Scheme 4). Unfortunately, these isomers could not be separated by either prep TLC or column chromatography.

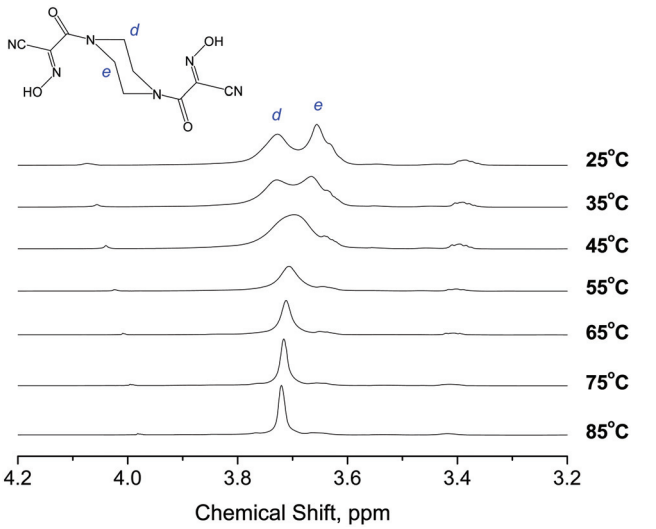

Fig. 1 Stacked plot of fragments of ^1H NMR spectra of **2** in the region of piperazine –CH_2– groups in DMSO-d_6 solution at variable temperatures.

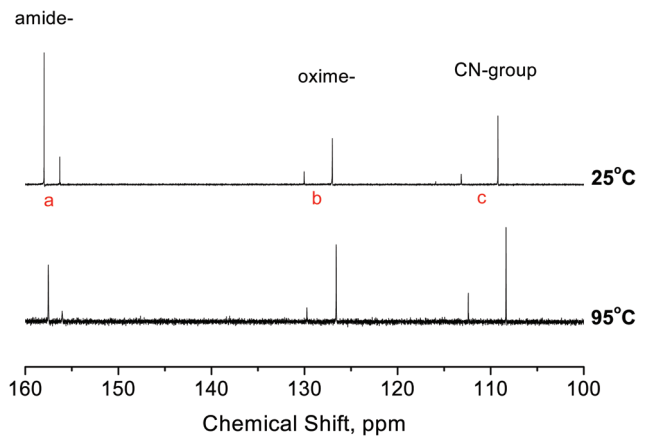

Fig. 2 $^{13}C\{^1H\}$ spectra of **2** in the *downfield* region of sp^2/sp carbons at high and low temperatures. Signals of two different geometrical isomers are: *syn–syn* (lower intensity) and *anti–anti*.

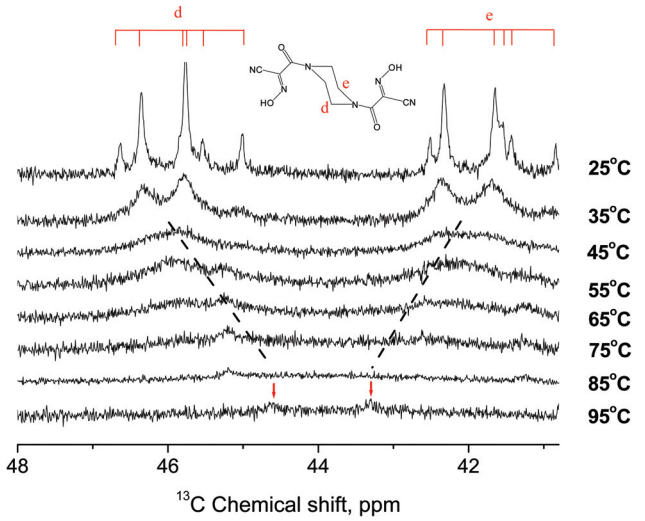

Fig. 3 Stacked plot of fragments of $^{13}C\{^1H\}$ NMR spectra of **2** in the region of $-CH_2-$ groups in DMSO-d_6 solution at variable temperatures. The appearance of two non-equivalent ***d***, ***e*** carbon atoms is due to the contribution of the amide form **II** (Scheme 5).

Along with the issue of the presence of a mixture of three geometrical isomers, a significant contribution of the form **II** (Scheme 5) to the overall electronic structure of H_2BiPipCO was found. This form prevents rotation around the C–N amide bond in the studied temperature range of 25–95 °C, due to the bond's partial double bond character. Therefore, a complex spectroscopic pattern in both ^1H and $^{13}C\{^1H\}$ NMR spectra of **2** was observed (Fig. 1–3) due to the total chemical non-equivalence of all protons and carbon atoms in the compound. The oxime proton appears as a highly de-shielded broadened two-component signal at 14.28 and 14.20 ppm which evidenced the difference in chemical shifts between *syn–syn* and *anti–anti* isomers. A moderate heating to ~50 °C leads to the disappearance of these signals from the spectrum due to the fast exchange (ESI 9†).

The signals of the **d–e** protons of the piperazine ring at room temperature appeared as broadened, poorly resolved peaks (Fig. 1). There are several conformations of the piperazine group with the *axial–equatorial* protons in cyclic "chair–boat" systems (Scheme 6). Heating the solution of **2** to +95 °C leads to the methylene groups **d** and **e** signals' coalescence and then narrowing, which indicates the range of fast dynamic exchange between "chair–boat" conformations with their time averaged position (Fig. 1).

The $^{13}C\{^1H\}$ NMR spectrum of **2** was not trivial and indicated coexistence of several geometrical isomers, which are diastereomers (ESI 13†). In order to better understand the origin of different signals and their dynamics, a series of variable temperature experiments were performed.

Although bulk material **2** according to the TLC is most likely a mixture of three isomers (*anti–anti*, *anti–syn*, and *syn–syn*; Scheme 4), there are only *two* sets of signals in the downfield area (Fig. 2; ESI 13†). These signal the amide-, oxime- and nitrile-group carbon atoms – ***a***, ***b*** and ***c*** respectively – that were unambiguously assigned based on previously published data[24–28] (Fig. 2). The two sets of signals imply the coexistence of the *syn–syn* and *anti–anti* isomers, and an overlap of signals of the *syn–anti* isomer with the other two (Scheme 4).

The ratio between the *syn–syn* and the *anti–anti* orientation of the oxime group was roughly estimated from the intensities of the signals in $^{13}C\{^1H\}$ NMR spectra, albeit not very accurate due to non-quantitative nature of conducted NMR experiments, and was found to be ~4 : 1 at +25 °C (Fig. 2). Heating of a DMSO-d_6 solution of the compound **2** to +95 °C does not drive a complete conversion of one isomer into another, but does increase the ratio change between the isomers (Fig. 2). This finding correlates with previous observation of the cyanoxime *syn*-isomer partial conversion into the *anti*-isomer at elevated temperatures.[25,29] The $^{13}C\{^1H\}$ NMR spectra of **2** at room temperature showed two groups of *six* signals in the area of aliphatic sp^3 carbon atoms (Fig. 3; ESI 13†). The presence of the two groups of signals in the spectrum at 25 °C indicates the lack of symmetry and rotation around the C–N amid bond in **2**.

Thus, two carbon atoms **d** and **e** of the piperazine group are chemically non-equivalent because of the different orientation of the >C═O fragment of the amide group. Indeed, heating of the sample to +95 °C confirms that assignment: only two temperature-broadened signals are observed, as expected (Fig. 3, bottom trace). The amide groups in this compound are *planar* have partial double bond character (as was established by the X-ray analysis; see description below) and, therefore, "frozen" from rotation. Consequently, all carbon atoms in the piperazine ring are non-equivalent. Variable temperature $^{13}C\{^1H\}$ NMR spectra evidence the presence of the dynamic boat–chair equilibrium (Scheme 6). Observed spectroscopic changes at different temperatures are reversible. Thus, six different conformations of the ring for three geometrical isomers arise from two chemically non-equivalent carbon atoms of the piperazine group (Scheme 4, Fig. 3). Their exact assignment is not possible without further extensive

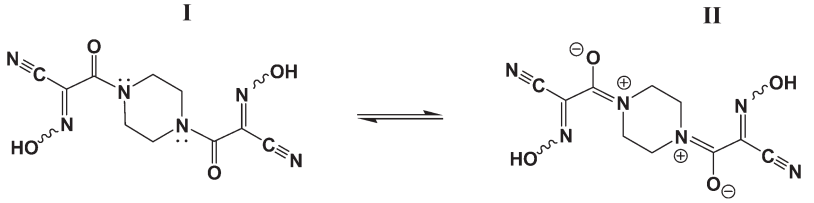

Scheme 5

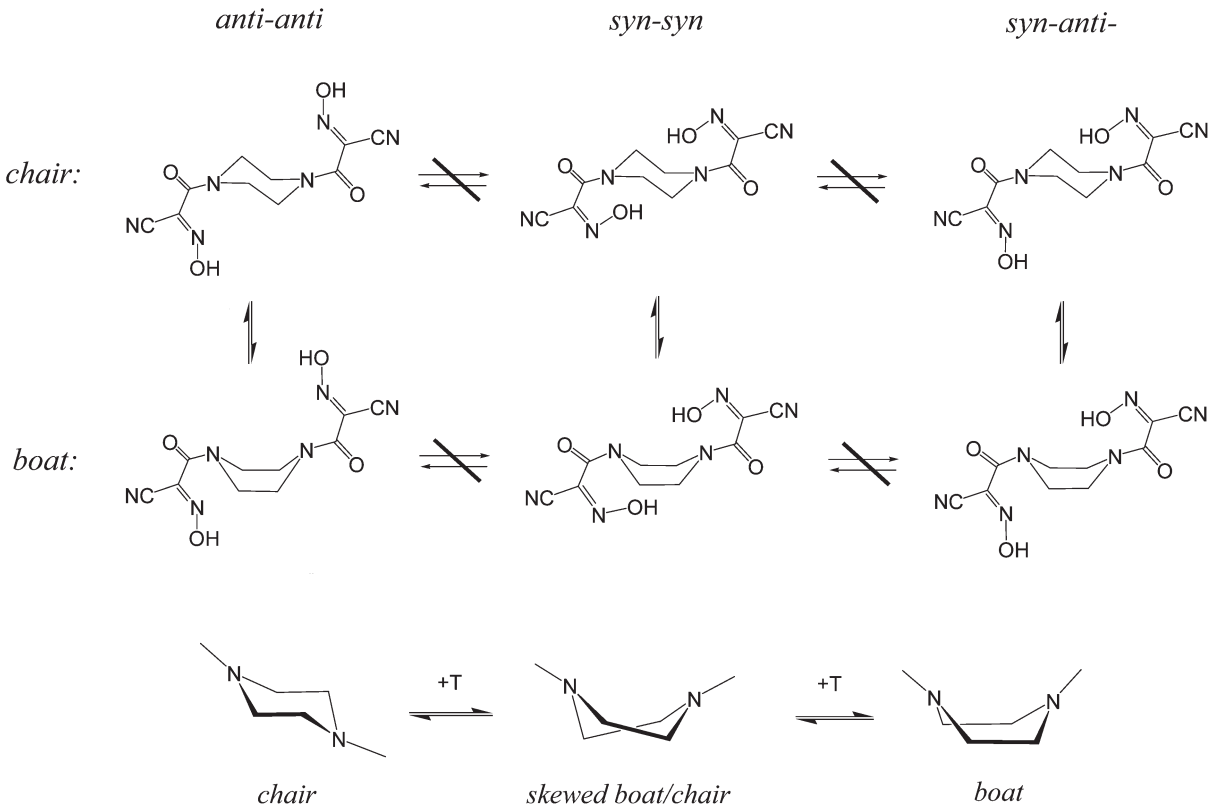

Scheme 6

experimental studies and appropriate theoretical calculations, which were out of scope of this work.

The deprotonation of **2** with the formation of the dianion in disodium salt **3** leads to a different NMR spectroscopic signature, which is presented and discussed in ESI 15.†

NMR spectra of products of crystallization of 2. The NMR spectra discussed above were obtained from a bulk, white, powdery material of **2** obtained directly from the reaction shown in Scheme 3. Slow crystallization of a 1 : 1 ethanol–acetone solution of a bulk sample of **2** at +4 °C afforded ~10% of clear crystals (minor fraction 2) that appeared on top of a white compact powder (major fraction 1) (ESI 14†). The $^{13}C\{^1H\}$ NMR spectra were recorded from both specimen and indicated that clear crystals represent a mixture of *syn–syn* and *anti–anti* isomers (Scheme 4) at almost equal amounts (ESI 14†). This was confirmed by crystallographic data presented below and indicated that crystals contained 51.2% of *syn–syn* and 48.8% of anti–*anti* isomers. Thus, an ability of the biscyanoxime **2** to co-crystallize in one unit cell two *geometrical isomers* is due to similar H-bonding that allows packing of two different molecules into the crystal. This implies very similar energies and geometrical arrangements of atoms involved in formation of such H-bonds. The second, major, white powdery amorphous specimen after prolonged crystallization represents almost a pure (>90%) *anti*-isomer (ESI 14†).

Thermodynamic calculations. Recorded variable temperature ^1H and $^{13}C\{^1H\}$ NMR experiments in DMSO-d_6 in the range from +25 to +95 °C were used to calculate some thermodynamic parameters of **2**. The heating of the sample causes a convergence of the ^1H and ^{13}C signals of the CH_2– groups of the piperazine, with the coalescence temperature of ~45 °C (Fig. 1 and 2). The value of the free energy $\Delta G^{\neq}$ for the process was calculated using eqn (8) and (9),[30] which was found to be 30.6 ± 0.2 kJ mol^{-1}.

$$k_c = \pi\frac{\sqrt{2}}{2}(\nu_a - \nu_b), \quad (8)$$

where k_c is the exchange rate constant at the coalescence T_c (K) of signals ν_a and ν_b

$$k_c = \chi\left(\frac{k_B T_c}{h}\right)e^{\left(\frac{-\Delta G^{\neq}}{RT_c}\right)} \quad (9)$$

where k_B is Boltzmann's constant, h is Planck's constant, and χ is a transmission coefficient = 1.

The obtained value of 30.6 kJ mol^{-1} for the piperazine ring boat–chair conformational changes is much larger than that for the cyclohexane and related aliphatic ring systems.[30] This is a reflection of significant increase in the rigidness of the functionalized piperazine. The ^{13}C signals from the carbon atoms other than the piperazine group in **2** do not converge (Fig. 2) because they are not conformers (boat/chair), but represent *individual geometric isomers* (*anti–anti*, *syn–anti*, *syn–syn*; Scheme 4; ESI 13†) with much higher rotation barrier energy.

The values of $\Delta G^{\neq}$ for the amide-bond rotation were reported to be 67.2, 72.6 and 64.9 kJ mol^{-1} for the 2-oximino-2-cyano-acetamide (HACO),[26] 2-oximino-2-cyano-*N*,*N*′-dimethylacetamide (HDCO),[26] and 2-oximino-2-cyano-*N*-piperidine (HPiPCO)[25] respectively.

UV-visible spectroscopy of the bis-cyanoxime ligand 2 and its dianion in 3. The UV-visible spectra of **2** and **3** conform to those typical of cyanoximes. The vast majority of protonated cyanoximes, with the exception of HTCO,[31] HBOBO,[24] and HBTCO,[32] are colorless compounds[27] that normally show two bands of $\pi \rightarrow \pi^*$ transitions at 220–230 nm and 270–300 nm in the UV region of the spectrum. The deprotonation of the cyanoxime **2** leads to the formation of yellow-colored solutions, due to the $n \rightarrow \pi^*$ transition in the nitroso-chromophore in the visible part of the spectrum (Fig. 4A). The dianion is stabilized because of the contribution of several resonance forms (ESI 16†). Also, the dianion of **2** exhibits a pronounced negative solvatochromism: the λ_{max} difference between spectra in MeOH and DMF is 88 nm (5013 cm^{-1}; 59.9 kJ mol^{-1} or 14.3 ccal mol^{-1}) (Fig. 4B). Such a large effect is attributed to the formation of a strong H-bond between protic solvents, such as methanol, and a deprotonated bis-cyanoxime anion.[33]

The H_2BiPipCO (**2**) and its disodium salt **3** do not fluoresce, either in solutions or in a solid state. This property will be very useful during our investigation of lanthanide and Ru(III) luminescent coordination-polymeric complexes, which we plan to carry out in the near future, since metal-based emission will not obstruct or interfere with the emission of the organic part of the framework.

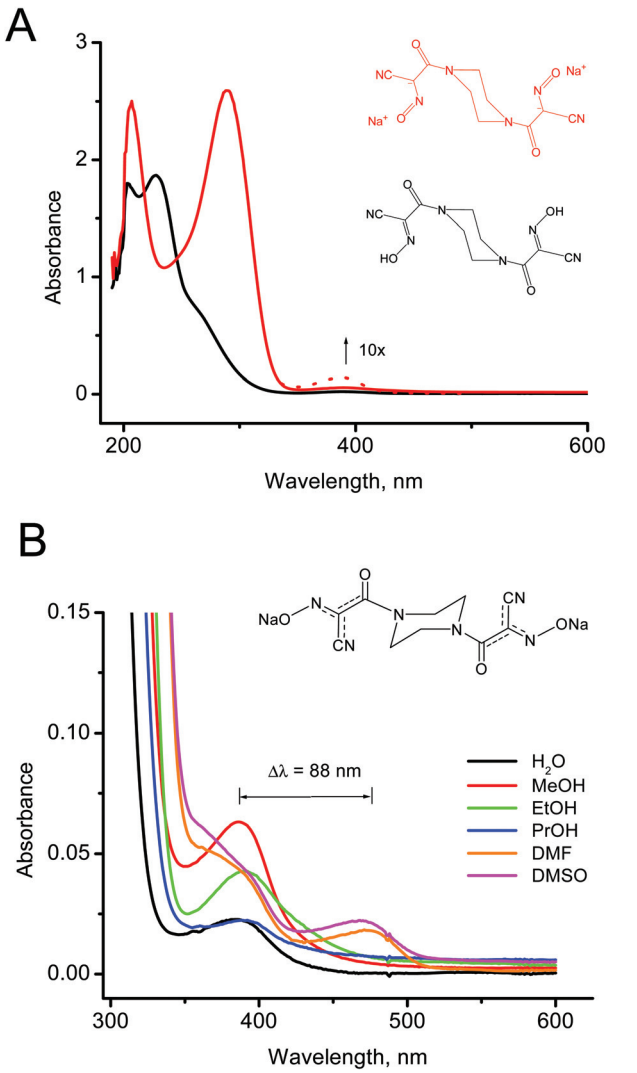

Fig. 4 Spectra of the protonated (**2**) and deprotonated (**3**) forms of H_2BiPipCO in the UV-visible region in ethanol (A), and solvatochromatic series for Na_2BiPipCO (**3**) in different solvents (B); T = 296 K, 1 cm quartz cuvette.

Solid state studies: structures and IR-spectra

Crystal structure of H_2BiPipCO, 2. Clear colorless crystals of the bis-cyanoxime **2** were grown from an aqueous/ethanol solution upon slow evaporation of solvents at +4 °C. All the crystals of **2** that were inspected for the X-ray analysis were non-merohedral twins, and details of the twin workup are presented in ESI 3.† The crystal structure of **2** represents a rare case of a co-crystallization of two geometrical isomers at close to 1 : 1 ratio (*syn–syn* 51.2% to *anti–anti* 48.8%, to be exact), which occurred only due to the demand for crystal packing requiring a similar H-bonding pattern (Fig. 5 and 6; ESI 17†).

The manifestation of the presence of both isomers in one unit cell in the crystal lattice appears as a two-positional disorder (Fig. 5), and often was confused as such in several previous publications.[34] The disorder commonly observed in crystal structures is due to the possibility of a group of atoms, or a molecule to adopt different positions in space, and is directly related to their rotation around one chemical bond, or reflection through the plane of symmetry, or inversion center at special positions.[35] The chemical identity of disordered species is the same: there are no spectroscopic differences between disordered species when they are in solution. The principal difference between co-crystallized isomers and other disordered molecules is that the former represent *chemically different species* that possess *spectroscopically different signatures.* Co-crystallized molecules, that happened to be present in one lattice in the crystal, fulfill the demand for close packing using H-bonding or other forces.[36] When such

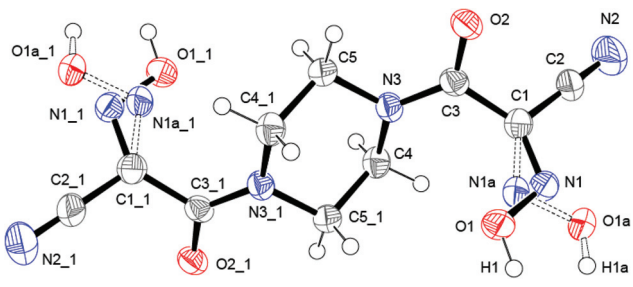

Fig. 5 Molecular structure and numbering scheme of the grow fragment in the structure of H_2BiPipCO showing *syn*-/*anti*-isomers disorder in the structure. The sym-code #1 (for the inversion center): –*x*, –*y*, –*z*. Here and further an ORTEP drawing at the 50% thermal ellipsoids probability level.

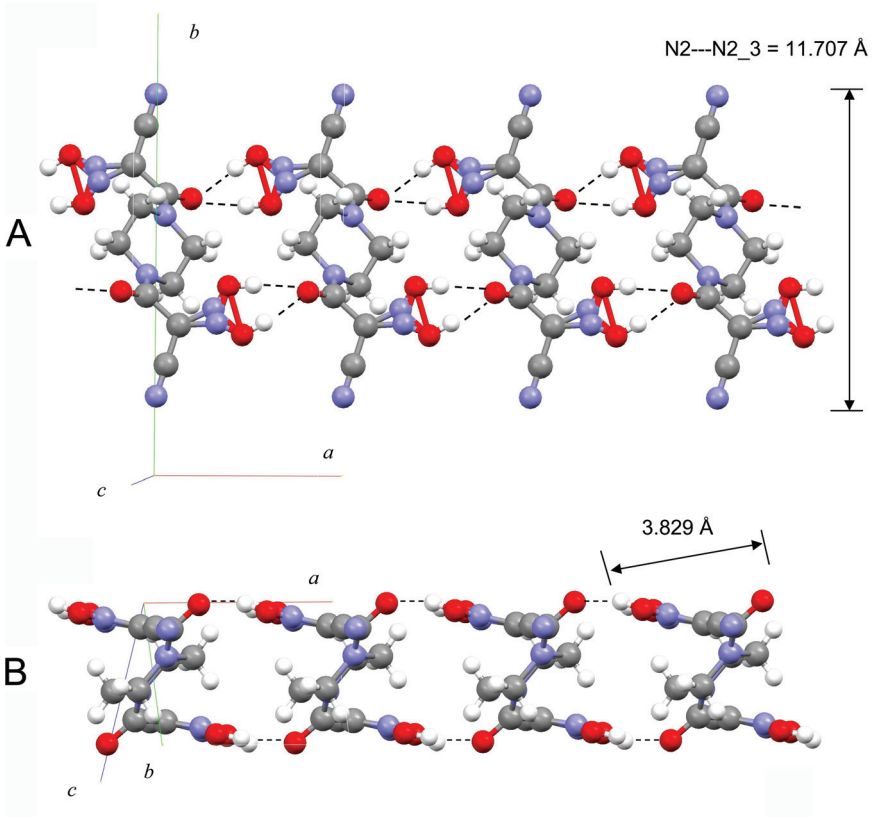

Fig. 6 Organization of the H_2BiPipCO structure: two views of H-bonded puckered ribbons along the *a*-axis. Hydrogen bonds are shown as dashed lines. The width of the sheet is of the nano-scale size (A), while the "thickness" of the sheet is 3.829 Å (B). Coloring scheme: grey – C, blue – N, red – O, white – H.

specimen is dissolved, the NMR spectra clearly demonstrate different chemical shifts for atoms in both isomers.[27a] There are instances when temperature increase can facilitate a conversion of one (*syn*- or *anti*-) isomer into another,[25] but most often it is not the case.[29] This observation provides clear distinction in terminology between the conformer and the isomer: the former undergoes changes in its conformation with the temperature change, while the latter may not undergo changes in its geometry at all. Typically oximes and cyanoximes, in particular, crystallize separately as individual isomers.[27,37,38] However, it has been shown earlier that in some rare cases a co-crystallization of both isomers is possible, as was found in the structures of 3-fluorophenyl-cyanoxime[28] (ESI 18†), 1,3-bis-cyanoximebenzene[15] (ESI 19†), 2-oximino-2-cyano-*N*-piperidineacetamide (ESI 20†), 2-benzimidazolyl (cyanoxime)[38] (ESI 21†). Two isomers were also recently found in the structure of the K^+ salt of the nitro-oxime.[39] Moreover, coordination compounds of both *syn*- and *anti*-geometrical isomers were shown to co-crystallize in one unit cell in a single crystal.[38] Some of the most recent examples include Ag(I) cyanoximates (depicted in ESI 22,23†), while the Tl(I) mixed isomers complex with 2-thiazoline(cyanoxime) was reported[40] in 1995.

All bond lengths and valence angles in both isomers in the structure of **2** are typical of cyanoximes. One interesting peculiarity of this crystal structure is the practically planar arrangement of the amide fragment with a 0.046 Å deviation from the mean plane of the O2–C3–N3–C4–C5 atoms. However, as far as the individual planes O2–C3–N3 and N3–C4–C5 in the amide group are concerned, the small dihedral angle between them is equal to 10.01°. This finding explains the complexity of the NMR spectra of **2**, associated with the inability of the piperazine group to rotate around the amide bond due to its partial double-character: C3–N3 = 1.327(4) Å (Table 2). As a result, the non-equivalence of carbon atoms ***d*** and ***e*** is observed due to their different proximity to the carbonyl group and different shielding resulting in ~4 ppm chemical shift difference (Fig. 2 and 5). The crystal structure of **2** represents an interesting 2D framework of molecules that are H-bonded along the *a*-axis and shaped as puckered sheets (Fig. 6). The interaction between the sheets has both van der Waals and electrostatic character since there are relatively short and well-oriented C–H···N contacts between the piperazine methylene groups and cyano-groups of neighboring sheets (ESI 17†). In summary, the crystal structure of **2** is another example of co-crystallization of *syn–syn*/*anti–anti* isomers in the same unit cell because of the very similar energies for both isomers and crystal packing demands.

Unfortunately, despite numerous attempts we were unable to grow crystals of transition metal complexes that include biscyanoxime ligand **2** which were suitable for the X-ray analysis. Therefore, the characterization of metal derivatives of this new

bis-cyanoxime ligand is limited in the presented work only to the description of the Tl(I) complex.

Crystal structure of Tl_2(BiPipCO), 4. Crystals of **4** were obtained by slow cooling the hot aqueous solutions leading to single crystals suitable for structure determination (ESI 24†). Thus, several batches of crystals were grown using this technique, but in most cases the overall quality of crystals was poor: they were either twinned/multi-domain specimen, or opaque, indicating some internal imperfections, which may be referred to as occluded micro-bubbles of CO_2 trapped inside the crystals. As mentioned in the Experimental section, several intense residual Q-peaks in close proximity to the metal center were observed on the electron density map in the structure of **4** (ESI 5†). They are attributed to the "ripples" of electron density near the heavy atom in the structure. In well determined structures of small organic compounds the values of residual electron density are expected to be in the range of 0.26–0.35 e $Å^{-3}$. However, the presence of a heavy atom such as Tl (Z = 81), that is ~13 times heavier than carbon (Z = 6), increases an order of magnitude residual electron density close to the metal. For example, values of residual electron density were observed to be 1.59 e $Å^{-3}$ in Tl(I) nitrosodicyanomethanide,[41] 2.66 e $Å^{-3}$ in Tl(I) 3-pyridyl-cyanoxime,[42] 3.62 e $Å^{-3}$ in Tl(I) 4-pyridyl-cyanoxime,[42] and 3.95 e $Å^{-3}$ in Tl(I) 2-benzthiazolylcyanxome.[24]

Prior to the description of the crystal structure of the obtained Tl(I) complex **4**, it is important to mention some reference distances[43] between the metal ion and N, O donor atoms of the ligands should be compared to the sum of ionic radii for Tl–O = 2.85 Å and Tl–N = 2.96 Å. When interatomic distances are shorter than the sum of ionic radii, this evidences some covalence in bonds between involved atoms. Also, Tl(I) has a $6s^2$ *inert electron pair* that, despite its supposedly spherical nature, shows pronounced spatial directionality.[44] Thus, it can often be visualized in crystal structures in an open cleft near Tl(I) centers.[45] Therefore, in numerous monovalent thallium complexes the $6s^2$ electron pair acts as a lone pair and as such it is frequently called a *stereochemically active* pair.[46,47] The molecular structure and the numbering scheme are shown in Fig. 7; while selected bond lengths and angles are presented in Table 2.

Compound **4** forms an interesting 3D coordination polymer that represents 1D columns interconnected *via* additional, longer Tl1–O2 contacts (Fig. 8A). There are two bonds shorter than the sum of ionic radii between Tl(I) and O1 atoms: 2.655 and 2.769 Å (Table 2), and three longer ones, electrostatic thallium–oxygen contacts at 2.894, 2.950 and 2.986 Å (ESI 25†).

The crystal structure of **4** is organized in such a manner that infinite 1D columns consist of a double-stranded ladder-type motif (Fig. 8D). The latter is built of two slightly different Tl_2O_2 rhombs that are adjacent at a 95.95° angle (ESI 24†). Therefore, three intermetallic distances can be found in these rhombs (4.276, 4.310 and 4.369 Å), but none of these is sufficient for consideration as a bond or metallophilic interaction.[48] The lone $6s^2$ pair of Tl(I) is stereoactive and can be envisioned occupying an open cleft between the longest

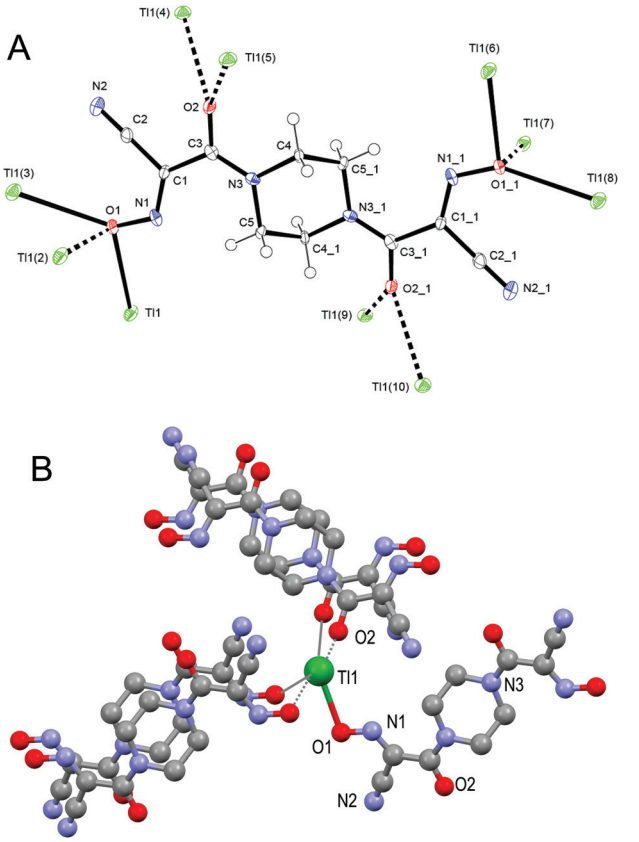

Fig. 7 (A) The GROW fragment in the structure of **4** showing one cyanoxime anion and five closest Tl-atoms as an ORTEP drawing at a 50% thermal ellipsoids probability level (the inversion center (#1: $-x, -y, -z$) is indicated as yellow x); symmetry codes for Tl centers: Tl1: x, y, z; (2): $1-x, 1-y, 1-z$; (3): $2-x, 1-y, 1-z$; (4): $2-x, -1/2+y, 3/2-z$; (5): $1-x, -1/2+y, 3/2-z$; (6): $1-x, 1-y, 2-z$; (7): $x, y, 1+z$; (8): $x-1, y, 1+z$; (9): $x, 3/2-y, 1/2+z$; (10): $x-1, 3/2-y, 1/2+z$. (B) One Tl-atom and its nearest five cyanoxime anions; dotted lines show long, electrostatic contacts. H-atoms are not shown for clarity.

Tl1···O1 (2.986 Å) and Tl1···O2 (2.950 Å) contacts (ESI 25†). The anion **2** adopts a *trans–anti* configuration and a slightly shorter N1–C1 bond than an N1–O1 bond, which indicates the *oxime* character of the anion (Table 2). The piperazine group adopts the chair conformation in the structure of **4**, with the rest of the bond lengths and angles in the structure being normal for Tl(I) cyanoximates.[11]

The bis-cyanoxime $BiPiPCO^{2-}$ dianion by design is a polydentate ligand that may exhibit numerous binding modes; some of which are presented in Scheme 7. The oxygen sites binding coordination type **4** was found in the crystal structure of Tl_2(BiPipCO). As a building block the bis-cyanoxime may employ the bridging modes **1–3** in organoantimony(V) and in organotin(IV) complexes. The bridging type **5** for the ligand could be found in the structure of the silver(I) complex. Transition metals such as Cu, Ni, Co, Fe or Pd, Pt, and lanthanoids most likely favor coordination modes **6–8**, with the formation of five- and six-membered chelate rings (Scheme 7).

Infrared spectra. The FT-IR spectra of the compounds synthesized in this work are summarized in Table 3. A significant redistribution of electron density in the ligand upon

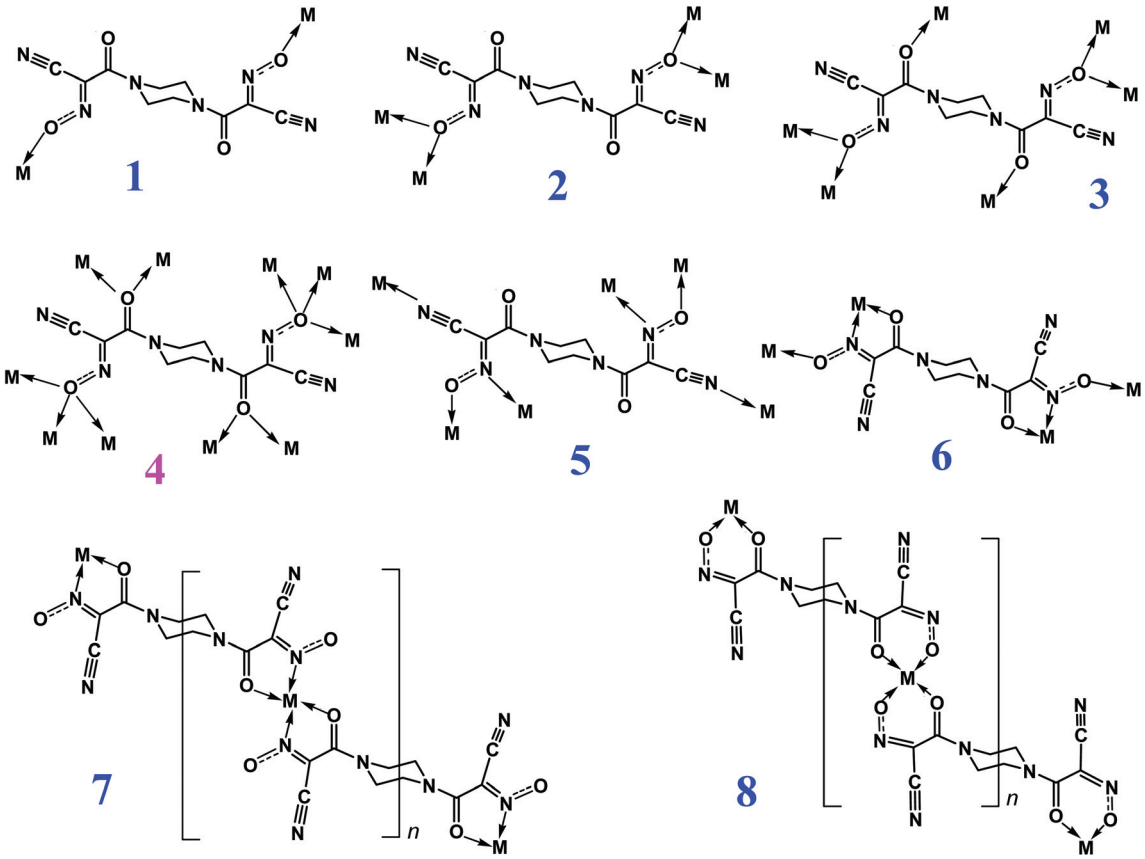

Scheme 7

deprotonation (as in the ionic disodium salt **3**) and subsequent coordination to heavy metal centers is observed. This process results in a shift of the stretching vibrations of nitroso- and carbonyl-groups in the IR-spectra.

The coordination of the carbonyl group of the bis-cyanoxime dianion to the metal centers in complexes **4** and **5** is evident from lowering of the ν(C=O) vibrations compared to that in the protonated ligand **2** and its disodium salt **3**. An increase in energy of the vibrations of the oxime fragment indicates its involvement with respect to the coordination to Tl(I) and Ag(I). In the latter complex, peak shifts are similar to other reported silver(I) cyanoximates.[33,41] Silver complexes generally show different bridging binding modes when compared to thallium complexes.[11] Transition metal Ni-triad complexes presumably contain the bis-cyanoxime $BiPiPCO^{2-}$ dianion in chelating binding modes (**6**, **7** or **8** in Scheme 7) similar to the one previously observed in other metal compounds that include Ni,[49] Pd and Pt.[25,50] However, without X-ray analysis data, binding modes and structures of these complexes can be only suggested.

Conclusions

(1) A new bis-cyanoxime ligand was synthesized in high yield as a mixture of structural isomers using a room temperature nitrosation reaction with gaseous methylnitrite under basic conditions. This compound – di-*N*,*N*′-(2-cyano-2-oximinoacetyl)piperazine – was characterized by NMR, UV-visible spectroscopy, X-ray analysis and pK_a measurements.

(2) The prolonged crystallization of the bis-cyanoxime leads to a co-crystallization of the mixture of *syn–syn*/*anti–anti* isomers (51.2% and 48.8%), and a major product as a white, amorphous, and practically pure *anti–anti* isomer. The X-ray structure of di-*N*,*N*′-(2-cyano-2-oximinoacetyl)piperazine shows that in both geometrical isomers the cyanoxime group adopts a *trans*- configuration in the molecule with respect to a practically planar C(O)N(C,C) amide fragment.

(3) Deprotonation of the bis-cyanoxime with a base leads to a bright-yellow dianion in water and alcohol solutions, which changes the color to pink in DMF and DMSO, showing pronounced solvatochromism. No fluorescence was detected either from a protonated organic ligand or from its dianion. Thus, the material is suitable for making Ru or lanthanide based luminescent frameworks without undesirable interference with the emission from the organic ligand.

(4) Several metal derivatives (Na, monovalent Ag, Tl and bivalent Ni, Pd, Pt) of the first bis-cyanoxime were synthesized and characterized. The crystal structure of a di-thallium complex of bis-cyanoxime was determined and showed the formation of a 3D coordination polymer in which the dianion exhibits a bridging function and acts as a formally decadentate

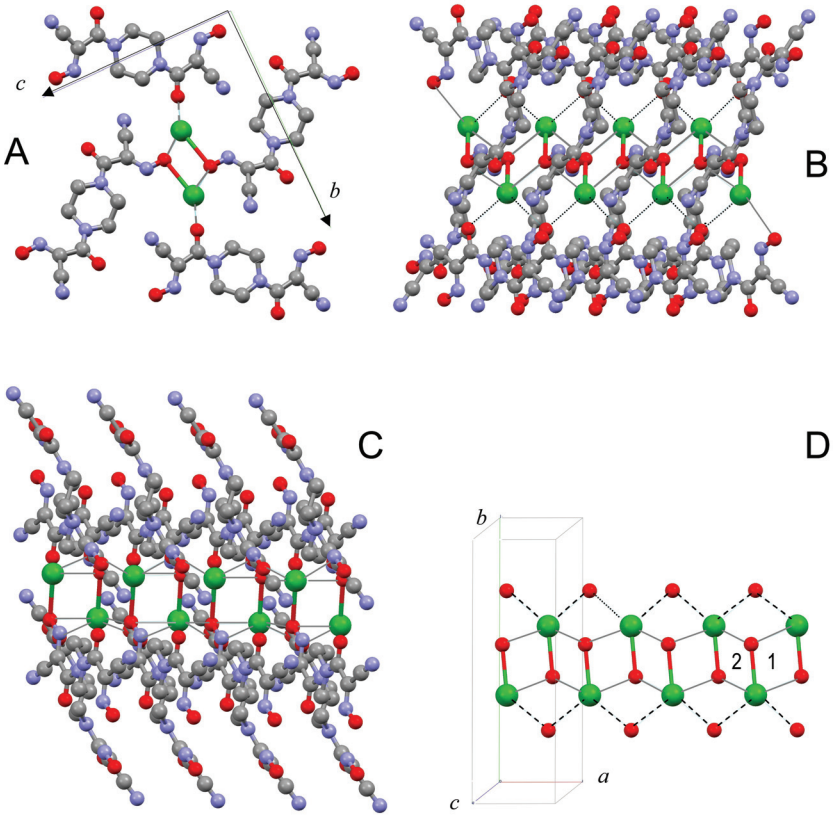

Fig. 8 Organization of crystal structure of **4**: A – prospective view of three unit cells along *a*; B and C – prospective views of three unit cells along showing puckered sheets of the coordination polymer, D – view along *c* of only the $Tl_2O_2'O_2''$ double-stranded (ladder type) motif. H-atoms are not shown for clarity. Dotted lines indicate longer contacts between O and Tl atoms.

Table 3 IR-spectroscopic data for solid samples of $BiPipCO^-$-containing compounds

	Assignment of frequencies, cm^{-1}					
Compound	$\nu^{as}CH$	$\nu^{s}CH$	$\nu(C{\equiv}N)$	$\nu(C{=}O)$	$\nu^{s}NO$	$\nu^{as}NO$
2, $H_2BiPipCO$	3175	2971	2232	1625	1047	1176
	3124	2813	2243			
3, $Na_2BiPipCO\ 4H_2O$	2925	2859	2218	1617	1136	1276
4, $Tl_2BiPipCO$	[a]	[a]	2207	1576	1170	1310
5, $Ag_2BiPipCO{\cdot}2H_2O$	[a]	[a]	2206	1585	1215	1340
			2228			
6, $NiBiPipCO{\cdot}4H_2O$	2926	2865	2218	1586	1172	1291
7, $PdBiPipCO{\cdot}4H_2O$	2925	2860	2213	1558	1154	1291
8, $PtBiPipCO{\cdot}5H_2O$	2920	2865	2213	1569	1159	1286

[a] C–H bands in silver and thallium compounds are obscured by the mulling agent.

ligand. Di-*N*,*N*′-(2-cyano-2-oximinoacetyl)piperazine demonstrated great potential as a semi-rigid bifunctional building block for the metal–organic frameworks, useful for coordination chemistry and crystal engineering.

Acknowledgements

NNG is very grateful to the Research Corporation (award CC6598) for support, and to Mrs Alex Corbett, Dr Olga Gerasimchuk for technical help. CC is thankful to the MSU Graduate College and the Department of Chemistry for financial support of his graduate work.

References

1 (*a*) C. Janiak, *Dalton Trans.*, 2003, 2781–2804 (and references therein) (*b*) A. U. Czaja, N. Trukhan and U. Müller, *Chem. Soc. Rev.*, 2009, **38**, 1284–1293 (and references

therein) (*c*) K. Sanderson, *Nature*, 2007, **448**(7155), 746–748; (*d*) S. F. Robert, *Science*, 2008, **319**(5865), 893.

2 (*a*) D. D. Perrin, *Organic Complexing Reagents*, Interscience, New York, 1964; (*b*) V. M. Peshkova, V. M. Savostina and E. K. Ivanova, *Oximes*, Nauka, Moscow, 1977.

3 (*a*) V. Pavlishchuk, F. Birkelbach, T. Weyhemuller, K. Wieghardt and P. Chaundhuri, *Inorg. Chem.*, 2002, **41**, 4405; (*b*) Y. Z. Voloshin, N. A. Kostromina and R. Kramer, *Clathrochelates: Synthesis, Structure and Properties*, Elsevier, Amsterdam, The Netherlands, 2002; (*c*) H. Miyasaka, T. Nezu, F. Iwahori, S. Furukawa, K. Sugimoto, R. Clerac, K.-I. Sugiura and M. Yamashita, *Inorg. Chem.*, 2003, **42**(15), 4501–4503; (*d*) K. J. Milios, T. C. Stamatatos and S. P. Perlepes, *Polyhedron*, 2006, **25**, 134–194; (*e*) K. M. McCauley, S. R. Wilson and W. A. van der Donk, *Inorg. Chem.*, 2002, **41**(22), 5844–5848; (*f*) A. Gupta, R. K. Sharma, R. Bohra, V. K. Jain, J. E. Drake, M. B. Hursthouse and M. E. Light, *Polyhedron*, 2002, **21**(23), 2387–2392; (*g*) V. Sharma, R. K. Sharma, R. Bohra, R. Ratnani, V. K. Jain, J. E. Drake, M. B. Hursthouse and M. E. Light, *J. Organomet. Chem.*, 2002, **651**(1–2), 98–104; (*h*) V. Yu. Kukushkin, D. Tudela and A. J. L. Pombeiro, *Coord. Chem. Rev.*, 1996, **156**, 333–362; (*i*) V. Yu. Kukushkin and A. J. L. Pombeiro, *Coord. Chem. Rev.*, 1999, **181**, 147–175.

4 (*a*) M. Megnamishi-Belombe, *J. Solid State Chem.*, 1979, **27**, 389; (*b*) J. W. Brill, M. Megnamisi-Belombe and M. Novotny, *J. Chem. Phys.*, 1978, **68**(2), 585–592; (*c*) K. Takeda, I. Shirotani and K. Yakushi, *Chem. Mater.*, 2000, **12**(4), 912–916; (*d*) T. Kamata, T. Kodzasa, H. Ushijima, K. Yamamoto, T. Ohta and S. Roth, *Chem. Mater.*, 2000, **12**(4), 940–945; (*e*) I. Shirotani, A. Onodera and Y. Hara, *J. Solid State Chem.*, 1981, **40**(2), 180–188.

5 (*a*) K. Yamamoto, T. Kamata, Y. Yoshida, K. Yase, T. Fukaya, F. Mizukami and T. Ohta, *Chem. Mater.*, 1998, **10**(5), 1343–1349; (*b*) T. Kamata, T. Fukaya, T. Kodzasa, H. Matsuda and F. Mizukami, *Synth. Met.*, 1995, **71**(1–3), 1725–1726; (*c*) Z. Sen, G. Günüs, I. Gürol, E. Musluoglu, Z. Z. Oztürk and M. Harbeck, *Sens. Actuators*, 2011, **160**, 1203–1209.

6 M. M. Olmstead and J. J. Sahbari, *Acta Crystallogr., Sect. E: Struct. Rep. Online*, 2003, **59**(11), o1648–o1649.

7 L. F. Chertanova, A. I. Yanovski, Y. T. Struchkov, V. F. Sopin and O. A. Rakitin, *Zh. Strukt. Khim. (J. Struct. Chem.)*, 1989, **30**, 112–116.

8 N. R. Streltsova, V. K. Bel'sky and Y. Z. Voloshin, *Acta Crystallogr., Sect. C: Cryst. Struct. Commun.*, 1993, **49**(3), 635–639.

9 G. Gervasio, D. Marabello and F. Bertolotti, *Acta Crystallogr., Sect. E: Struct. Rep. Online*, 2010, **66**(11), o2764.

10 (*a*) A. A. Mokhir, N. N. Gerasimchuk, E. V. Pol'shin and K. V. Domasevitch, *Russ. J. Inorg. Chem.*, 1994, **39**(2), 289–293; (*b*) N. N. Gerasimchuk, K. V. Domasevitch, A. A. Kapshuk and A. N. Tchernega, *Russ. J. Inorg. Chem.*, 1993, **38**(11), 1718–1722; (*c*) D. A. Fedorenko, N. N. Gerasimchuk and K. V. Domasevich, *Russ. J. Inorg. Chem.*, 1993, **38**(9), 1433–1436; (*d*) N. N. Gerasimchuk, V. V. Skopenko, V. V. Ponomareva and K. V. Domasevitch, *Russ. J. Inorg. Chem.*, 1993, **38**(6), 964–970; (*e*) N. N. Gerasimchuk and K. V. Domasevitch, *Russ. J. Inorg. Chem.*, 1992, **37**(10), 1163–1167.

11 N. Gerasimchuk, *Polymers*, 2011, **3**, 2–37.

12 (*a*) N. Gerasimchuk, T. Maher, P. Durham, K. V. Domasevitch, J. Wilking and A. Mokhir, *Inorg. Chem.*, 2007, **46**(18), 7268–7284; (*b*) L. Goeden, *The Synthesis, Characterization and Biological Activity Studies of Pt(II) and Pd(II) Disubstituted Arylcyanoximates*, MS thesis, Southwest Missouri State University, Springfield, USA, 2005; (*c*) D. Robertson, *Thallium(I) Coordination Polymers Based on Monosubstituted Arylcyanoximes*, MS thesis, Missouri State University, Springfield, USA, 2006.

13 (*a*) S. Soga, L. M. Neckers, T. W. Schulte, Y. Shiotsu, K. Akasaka, H. Narumi, T. Agatsuma, Y. Ikuina, C. Murakata, T. Tamaoki and S. Akinaga, *Cancer Res.*, 1999, **59**, 2931–2938; (*b*) S. H. Davidson, *2-Cyano-2-hydroximino-acetamides as Plant Disease Control Agents*, U.S. Patent 3957847, 1978; (*c*) V. V. Skopenko, G. K. Palii, N. N. Gerasimchuk, E. F. Makats, O. A. Domashevskaya and R. V. Rakovskaya, *Nitrosothiocarbamylcyanmethanide of Potassium or Sodium which Show Antimicrobial Activity*, USSR Patent 1405281, 1988; (*d*) G. K. Palii, V. V. Skopenko, N. N. Gerasimchuk, E. F. Makats, O. A. Domashevskaya and R. V. Rakovskaya, Bis-(nitrosothiocarbamylcyanmethanide) copper(II) or nickel(II) which exhibit antimicrobial activity, *USSR Pat.*, 1405282, 1988; (*e*) V. V. Skopenko, G. K. Palii, N. N. Gerasimchuk, O. A. Domashevskaya and E. F. Makats, Di-(nitroso-thiocarbamylcyanmethanide)-di-(pyridine)-copper which shows bacteriostatic activity towards Staphilococcus aureus, and method of preparation of the complex, *USSR Pat.*, 1487422, 1989; (*f*) K. Lin, Process for making 2-cyano-2-hydroximino acetamide salts, *U.S. Pat.*, 3919284, 1976; (*g*) A. Kuhne and A. Hubele, Method for the cultivation of plants employing R-cyanohydroximino acetamide derivatives, *U.S. Pat.*, 4063921, 1978; (*h*) H. Charlier and N. Gerasimchuk, Cyanoxime inhibitors of carbonyl reductase and methods of using said inhibitors in treatments involving antracyclines, *U.S. Pat.*, 7,727,967 B2, 2010.

14 N. N. Gerasimchuk and K. Bowman-James, Mixed donor ligands, in *Encyclopedia of Inorganic Chemistry*, ed. B. King, John Wiley & Sons, England, 1994, vol. 5, pp. 2254–2269.

15 S. Curtis, O. Ilkun, A. Brown, S. Silchenko and N. Gerasimchuk, *CrystEngComm*, 2013, **15**, 152–159.

16 N. Gerasimchuk, Synthesis, characterization and remarkable applications of light-insensitive silver(I), *cyanoximates*, in *New Trends in Coordination, Bioinorganic, and Applied Inorganic Chemistry*, ed. M. Melník, P. Segľa and M. Tatarko, Slovak University of Technology Press, 2011, pp. 106–113, ISBN 978-80-227-3509-4.

17 A. G. Lee, *The Chemistry of Thallium*, Elsevier Pub. Co, 1971, pp. 336.

18 *SAINT: Data Integration Program*, Bruker AXS, 1998.

19 (*a*) R. H. Blessing, *Acta Crystallogr., Sect. A: Fundam. Crystallogr.*, 1995, **51**, 33; (*b*) G. M. Sheldrick, *SADABS Area-detector Absorption Correction, 2.03*, University of Göttingen, Göttingen, Germany, 1999.
20 *Software Package for Crystal Structure Solution, APEX 2*, Bruker AXS, Madison, WI, 2009.
21 (*a*) L. Farrugia, *J. Appl. Crystallogr.*, 1997, **30**, 565; (*b*) M. N. Burnett and C. K. Johnson, *ORTEP III: Report ORNL-6895*, Oak Ridge National Laboratory, Oak Ridge, TN, 1996.
22 (*a*) J. Emsley, *The Elements*, Clarendon Press, Oxford, 1991; (*b*) J. Glaser, in *Advances in Inorganic Chemistry*, ed. A. J. Sykes, Academic Press, San Diego, 1995, vol. 43, p. 1; (*c*) H. Heydlauf, *Eur. J. Pharmacol.*, 1969, **6**, 340.
23 H. Charlier and N. Gerasimchuk, Cyanoxime inhibitors of carbonyl reductase and methods of using said inhibitors in treatments involving antracyclines, *U.S. Pat*, #7,727,967 B2, 2010.
24 O. T. Ilkun, S. Archibald, C. L. Barnes, N. Gerasimchuk, R. Biagioni, S. Silchenko, O. A. Gerasimchuk and V. Nemykin, *Dalton Trans.*, 2008, 5715–5729.
25 D. Eddings, C. Barnes, N. Gerasimchuk, P. Durham and K. Domasevich, *Inorg. Chem.*, 2004, **43**(13), 3894–3909.
26 K. V. Domasevitch, N. N. Gerasimchuk and A. A. Mokhir, *Inorg. Chem.*, 2000, **39**(6), 1227–1237.
27 (*a*) A. A. Mokhir, K. V. Domasevich, N. K. Dalley, X. Kou, N. N. Gerasimchuk and O. A. Gerasimchuk, *Inorg. Chim. Acta*, 1999, **284**, 85–98; (*b*) L. Goeden, N. Gerasimchuk, P. Durham, C. Barnes and J. F. Cannon, *Inorg. Chim. Acta*, 2008, **361**, 1983–2001.
28 D. Robertson, J. Cannon and N. Gerasimchuk, *Inorg. Chem.*, 2005, **44**(23), 8326–8342.
29 M. Giorgis, M. L. Loli, B. Rolando, A. Rao, P. Tosco, S. Chaurasia, D. Marabello, R. Fruttero and A. Gasco, *Eur. J. Med. Chem.*, 2011, **46**(1), 383–392.
30 A. J. Gordon and R. A. Ford, *The Chemist Companion (Handbook)*, John Wiley & Sons, New York, Chichester, Brisbane, Toronto, 1972.
31 V. V. Skopenko, O. A. Domashevskaya, N. N. Gerasimchuk and S. I. Tyukhtenko, *Ukr. Khim. Zh.*, 1986, **57**(7), 686–691.
32 K. V. Domasevitch, *Russ. J. Gen. Chem.*, 1997, **67**(9), 1572–1575.
33 N. Gerasimchuk, A. N. Esaulenko, K. N. Dalley and C. Moore, *Dalton Trans.*, 2010, **39**, 749–764.
34 (*a*) G. Dutkiewicz, H. S. Yathirayan, R. Ramachandran, S. Kabilan and M. Kubicki, *Acta Crystallogr., Sect. C: Cryst. Struct. Commun.*, 2010, **66**, o274–o278; (*b*) H. Book and T. Hauck, *Z. Naturforsch., B: Chem. Sci.*, 1994, **49**, 1012.
35 *Crystal Structure Refinement*, ed. P. Muller, Oxford University Press, I.U.Cr., 2006.
36 (*a*) A. I. Kitaigorodski, *Mixed Crystals*, Springer, 1984, pp. 388, ISBN-10: 0387109226; (*b*) T. Vries, H. Wynberg, E. van Echten, J. Koek, W. ten Hoeve, R. M. Kellogg, Q. B. Broxterman, A. Minnaard, B. Kaptein, S. van der Sluis, L. Hulshof and J. Kooistra, *Angew. Chem., Int. Ed.*, 1998, **37**(17), 2349–2354; (*c*) N. B. Bathori and L. R. Nassimbeni, *Cryst. Growth Des.*, 2010, **10**(4), 1782–1787; (*d*) G. I. Nikishin, A. T. Koritzky, S. V. Lindeman, R. G. Gerr, Yu. T. Struchkov and Eu. K. Starostin, *J. Am. Chem. Soc.*, 1989, **111**(26), 9214–9217; (*e*) A. W. Marsman, E. D. Leussink, J. W. Zwikker, L. W. Jenneskens, W. J. J. Smeets, N. Veldman and A. L. Spek, *Chem. Mater.*, 1999, **11**(6), 1484–1491; (*f*) F. J. Hoogesteger, L. W. Jenneskens, H. Kooijman, N. Veldman and A. L. Spek, *Tetrahedron*, 1996, **52**(5), 1773–1784.
37 L. Chertanova, C. Paskard and A. Sheremetev, *Acta Crystallogr., Sect. B: Struct. Sci.*, 1994, **50**, 708–716 (and references therein).
38 J. Morton, *Further Investigations of Silver(I) Cyanoximates*, M.S. thesis, 2010, pp. 138.
39 C. Reuter, J. M. Neudorfi and H.-G. Schmalz, *Acta Crystallogr., Sect. E: Struct. Rep. Online.*, 2010, **66**, m461.
40 K. V. Domasevitch, V. V. Skopenko and A. A. Mokhir, *Russ. J. Inorg. Chem.*, 1995, **40**(5), 781–786.
41 G. Glower, N. Gerasimchuk, R. Biagioni and K. V. Domasevitch, *Inorg. Chem.*, 2009, **48**(6), 2371–2382.
42 D. Marcano, N. Gerasimchuk, V. Nemykin and S. Silchenko, *Cryst. Growth Des.*, 2012, **12**, 2877–2889.
43 (*a*) CRC, *Handbook of Chemistry and Physics*, Boca Raton, Fl, 63rd edn, 1982–1983, p. F-179; (*b*) Atomic sizes and interatomic distances from a comprehensive source of information about properties of elements: available online at http://webelements.com
44 (*a*) G. Rayner-Canham, *Descriptive Inorganic Chemistry*, W. H. Freeman and Co., 2nd edn, 2001, p. 241; (*b*) G. L. Miessler and D. A. Tarr, *Inorganic Chemistry*, Prentice-Hall, 2nd edn, 1998, p. 244.
45 N. N. Gerasimchuk, A. N. Tchernega and A. A. Kapshuk, *Russ. J. Inorg. Chem.*, 1993, **38**(9), 1530–1534.
46 D. Robertson, C. Barnes and N. Gerasimchuk, *J. Coord. Chem.*, 2004, **57**(14), 1205–1216.
47 A. F. Cotton, G. Wilkinson, C. A. Murillo and M. Bohman, *Advanced Inorganic Chemistry*, John Wiley & Sons, New York, 6th edn, 1999.
48 (*a*) P. Pyykko and J. P. Desclaux, *Acc. Chem. Res.*, 1979, **12**, 276; (*b*) H. Schmidbaur, *Gold Bull.*, 2000, **33**(1), 3–10; (*c*) M. Kim, T. J. Taylor and F. P. Gabbai, *J. Am. Chem. Soc.*, 2008, **130**, 6332–6333; (*d*) T. P. Lin, C. R. Wade, L. M. Perez and F. P. Gabbai, *Angew. Chem., Int. Ed.*, 2010, **49**, 6357–6360.
49 (*a*) N. Gerasimchuk and N. K. Dalley, *J. Coord. Chem.*, 2004, **57**(16), 1431–1442; (*b*) V. V. Skopenko, Yu. L. Zub, R. D. Lampeka and V. K. Belskii, *Dokl. Akad. Nauk Ukr. SSR*, 1982, **B4**, 62–63.
50 J. Ratcliff, J. Kuduk-Jaworska, H. Chojnacki, V. N. Nemykin and N. Gerasimchuk, *Inorg. Chim. Acta*, 2012, **385**, 1–11.

